Optimizing energy and economic performance of solar-biomass systems for rural district heating: a technical and financial analysis

Xavier Jobard[1], Stefano Pauletta[1*], Alexis Duret[1] et Quentin Francois[1]

[1] HEIG-VD, Yverdon-Les-Bains (Switzerland)

Abstract

This article investigates the integration of large-scale solar thermal fields with biomass boilers for district heating (DH) in rural areas, aligning with the principles of 4th Generation DH. Using TRNSYS 17 software, the technical and economic aspects of this integration were analyzed. The technical assessment revealed high specific solar productivities over 850 kWh.m^{-2} for small solar fractions and a corresponding optimum specific volume of the Thermal Energy Storage (TES). The economic analysis demonstrated the viability of solar installations in various scenarios, with the potential for levelized costs of heat (LCOH) to be under 100 CHF/MWh. Overall, the study concludes that integrating solar thermal systems with wood chip boilers is technically feasible and financially advantageous. However, careful consideration of system configuration and financing is necessary for sustainable and high-performance solutions, ensuring optimal resource utilization and economic viability.

Keywords: Solar district heating, evacuated flat plate collectors, biomass boiler, economic assessment, levelized cost of heat.

***corresponding author stefano.pauletta@heig-vd.ch**

1. Introduction

District Heating Networks (DHNs) play a crucial role in advancing the adoption of renewable energy sources and harnessing local heat resources, such as low-temperature waste heat, making them an essential component of sustainable urban and rural energy strategies (Jessen et al., 2014; Tschopp et al., 2022). Traditionally, DHNs have relied heavily on fossil fuels and high distribution temperatures, due to reasons linked to the energy source, the transfer substation design and the type of serviced building and its heating system. But the high temperature regime typically adopted in the majority of DHN currently in operation (120 to 90°C) is not particularly favorable to the integration of lower temperature energy and local heat sources. Integrating renewable sources like solar, geothermal and biomass energy into DH networks can significantly improve its energy efficiency and sustainability (Jodeiri et al., 2022), but it requires, among other interventions, lowering the DHN operating temperatures to maximize the renewable energy share, which in turn can further improve the DH network efficiency as distribution heat losses are reduced. Modern buildings, furthermore, feature lower heating energy needs and are often compatible to the lower temperature regimes due to larger heat distribution systems. For example, from the house radiators of the past, needing supply temperatures in the 70-60°C range, nowadays, for new constructions, subfloor heating is frequently adopted, with supply temperatures typically around 38°C (Quiquerez et al., 2013).

In this context, the evolution towards the 4th Generation District Heating (4GDH) would mark a significant shift (Lund et al, 2014). These modern networks operate at lower temperatures, typically between 30-50°C, enhancing their ability to integrate diverse renewable energy sources, including solar thermal, geothermal, and waste heat from industrial processes. These lower operating temperatures not only reduce heat losses, but also align with the increased efficiency of contemporary building heating systems, paving the way for more resilient and eco-friendly energy infrastructures and communities (Jenssen et al., 2014). In this framework, Ruesch et al. (2020) have investigated the potential for low-cost solar heat production and integration with biomass in Switzerland, with specific configurations achieving costs competitive with those of fossil fuels. The report underscores the ecological benefits of using solar thermal energy to offset biomass use during summer, thus conserving wood resources for winter when renewable alternatives are limited. Similar conclusions are obtained by Jobard et Duret (2022) through numerical simulation, confirming that integrating solar heat production can reduce startup cycles for wood boilers, though marginal increases may occur during mid-season.

10.18086/eurosun.2024.09.08 Available at http://proceedings.ises.org

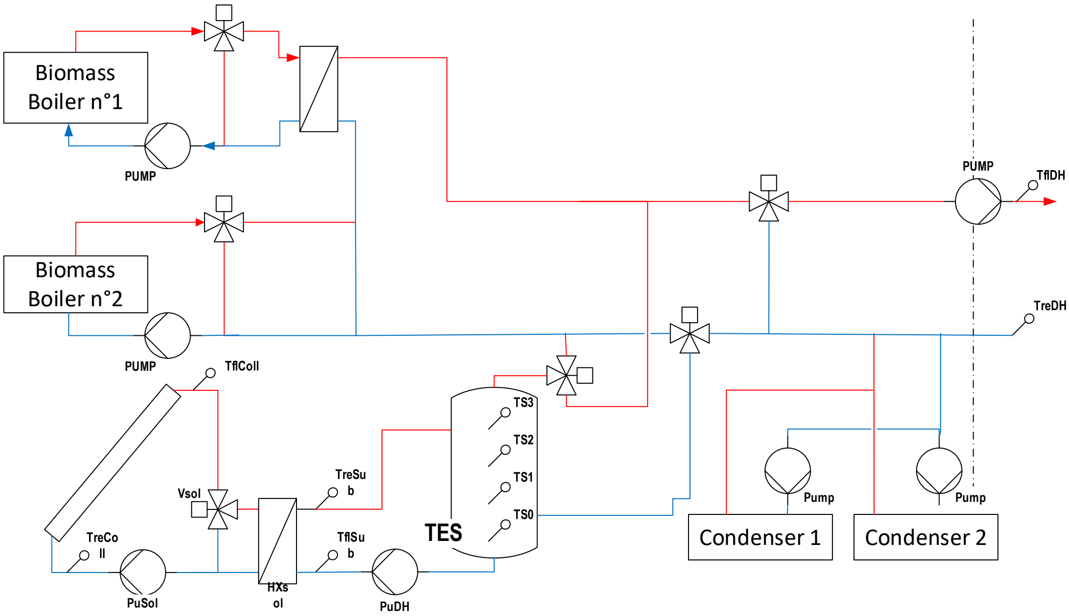

Figure 1: Simplified hydraulic diagram of the hybrid biomass-solar DH plant under study.

This paper aims at investigating the technical and economic performance of large-scale solar thermal plants combined with biomass boilers for DHNs in rural areas, by extending the analysis presented in Jobard et Duret (2022) to the case of evacuated flat solar collectors. In order to provide more realistic estimations, the original numerical model of the plant developed under TRNSYS and adopted to determine the impact of solar energy on the biomass boiler operability, was integrated with a TRNSYS model of a solar field made of 400 evacuated flat plate solar collectors manufactured by TVP Solar SA. This latter model, validated on the monitoring data of the SDH plant of Geneva, has been extrapolated to the lower operating temperatures typical of the 4th generation DH to precisely estimate the performance figures required for the economic analysis.

2. Methodology

The energy optimization and the investigation of the economic performance of solar-biomass systems for rural district heating has been carried out through a technical, economic and financial analysis. The technical analysis adopted TRNSYS 17 software to model a district heating power station made of 2 wood-fired boilers, each equipped with a flue gas condenser, integrated to a solar thermal plant and a thermal energy storage (TES), see Figure 1. The numerical model for the wood-fired section of the plant equipped with a TES was validated in a previous study by Jobard et Duret (2022), while the solar field model validation has been described by Duret et al. (*in press*).

Several plant configurations were investigated to optimize the renewable heat production by varying the solar array size and the TES volume. A final economic analysis investigated the investment and operating costs in 3 scenarios selected based on their respective solar fraction. A series of key performance indicators was then computed to allow an economic comparison among the selected scenarios.

The technical assessment was based on the computation of a series of technical indicators (see CEA, 2018), in particular:

- The solar annual yield (Q_0,), which is the quantity of solar thermal energy collected by the power plant during 1 year of operation and injected into the TES or the DH, expressed usually in [MWh/y] or [kWh/y].
- The specific solar yield or specific heat production (spQ_0), computed as the ratio between the solar annual yield and the total aperture area of the solar collectors (i.e. the aperture area is the area through which light can enter the collector); it is expressed in [kWh/m^2/y].
- The solar fraction (SFr), which is an indicator representing the fraction of the total energy consumption satisfied by solar thermal energy. It is defined as the ratio between solar energy production

(in, e.g., [MWh/an]) and the total energy consumption of the plant in the same period (also in [MWh/an]); it is expressed in [%].

To carry out the economic analysis, on the other hand, the capital expenditures (CAPEX), or the investment costs, were considered, together with the plant operational expenditures (i.e., OPEX). A series of assumptions was made for the financial parameters of the economic analysis, like the nominal discount rate, the system lifetime, the market price for the auxiliary electricity consumption, the selling price for the heat injected by the plant on the DH network and energy price inflation rate. To assess the economic viability for each scenario, the following key performance indicators, selected again from CEA (2018), were computed:

- The levelized cost of heat (LCOH), which is defined as the constant energy price in real terms required for the revenues generated from the project to be sufficient to obtain an internal rate of return equal to the discount rate. When using nominal figures, this indicator returns the average nominal price required trough the project's life to generate the required nominal return (Aldersey-Williams et Rubert, 2019). The calculation formula is as follow:

$$LCOH = \frac{CAPEX + \sum_{t=1}^{n} \frac{OPEX}{(1+r)^t}}{\sum_{t=1}^{n} \frac{Q_0 (1-d)^t}{(1+r)^t}} \qquad \text{(eq. 1)}$$

  where CAPEX includes all the investment costs incurred at the beginning of the project (i.e., year 0); OPEX are the operational expenditures at year t; r is the nominal discount rate; Q_0 is the annual heat delivered by the power plant to the DH network in year *0* expressed in [MWh/y]; d is the rate of panel degradation, in [%/y]; t is the year under consideration; n is the plant's lifetime, in [y].

- The Payback Period (*PP*), which is the time needed to make the project profitable and to recover the initial investment. Expressed in [y], it gives the number of years after which the project's Net Present Value (NPV) becomes positive.

- The Profitability Index (*PI*), which measures the profitability of an investment. It corresponds to the value created for each euro spent on the investment and it is expressed in [%]. It is computed as the rate between the sum of discounted future cash flow and the initial investment.

- The Internal Rate of Return (*IRR*), which evaluates the profitability of an investment and is commonly adopted to compare investments projects. It is the discount rate at which the net present value (NPV) of all future cash flows (both incoming and outgoing) equals zero.

By comparing the scenarios based on these KPIs, it is possible to gain an insight of the overall profitability of each system and rank them based on their LCOH.

3. Simulation setup

The model developed under TRNSYS makes use of specific "types", computational modules dedicated to performing the simulation of a particular plant component or process. Figure 2a and Figure 2b show the TRNSYS model for the complete plant and for the solar part, respectively. Among the adopted types, it is

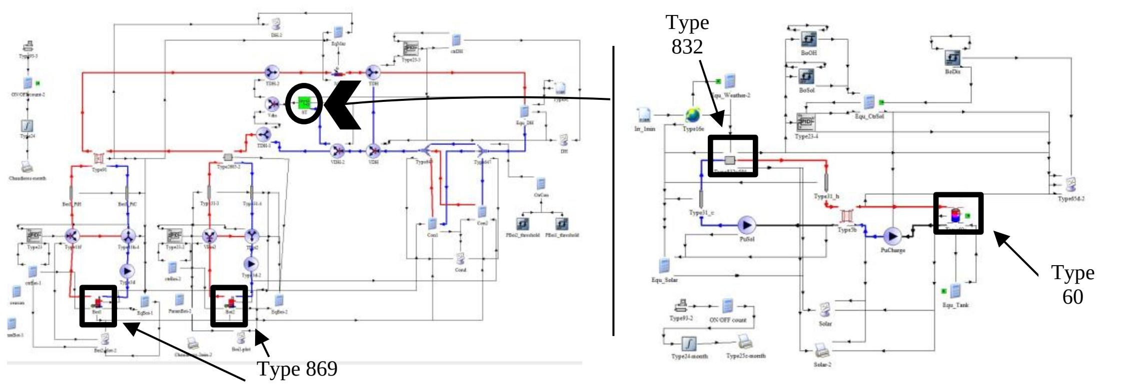

a) Overall TRNSYS model b) TRNSYS model for the solar field and TES

Figure 2: (a) General TRNSYS model for the hybrid biomass-solar DH plant; (b) TRNSYS model adopted for the solar field and integrated in the general model as a macro (black circle in (a)).

Table 1: Main characteristics of the modelled DH network

Modelled DH network parameter	Value
Annual total heat production, in [MWh/an]	5'830
Annual consumption for DHW production, in [%]	30
Nominal heating power @ -11°C, in [MW]	1.6
Nominal power for DHW production, in [kW]	400
No-heat temperature, in [°C]	16
Distribution heat losses, in [%]	10

worth noting the adoption of type 869 for the biomass boiler, type 832 for the solar collector and type 60 for the TES. The reader can refer to Jobard et Duret (2022) to find the detailed description of the TRNSYS model based on the DH network of the town « Les-Ponts-de-Martel », exploited since 2007 and located in Switzerland. On the other hand, the solar field model is derived from the one of the solar DH plant of Geneva, equipped with TVP Solar SA evacuated collectors. Duret et all (*in press*) describe in detail the numerical model and its validation against measurement data acquired at a 1-per-minute sampling rate. The validated model has been then extrapolated to the case of the "Les-Ponts-de-Martel" DH, in which the solar field operates at lower temperatures (i.e., while the Geneva operates at 95-80°C in summer, the temperature regime of the rural DH under consideration in the same season is as low as 70-45°C). Table 1 resumes the main features of the modelled DH network. For the current study, the meteorological data were derived by the service provided by MeteoSwiss, the Swiss Federal Office of Meteorology and Climatology, while the DH temperature and power profiles were taken directly from the monitoring data of the DH network of Les-Ponts-des-Martel.

4. Technical assessment

Once developed, the simulation model was used to evaluate the overall performance of the hybrid plant for several values of solar field aperture area, TES volume and solar fraction. Figure 3 shows the simplified but systematic procedure adopted to preliminary dimension the solar field and TES volume based on a target solar fraction value (Hiris 2022). For a given energy consumption, depending from the assumed solar fraction, the specific yield of solar collectors is estimated at an average value of 875 or 750 kWh/m^2/y, which allow grossly

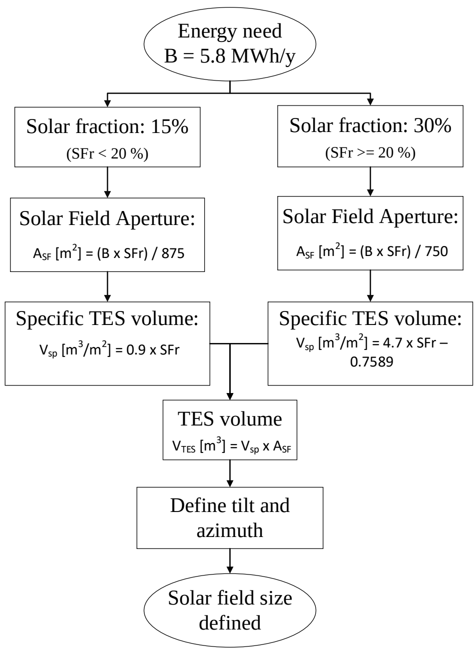

Figure 3: Simplified procedure followed for sizing the solar field area and the TES volume from a target solar fraction

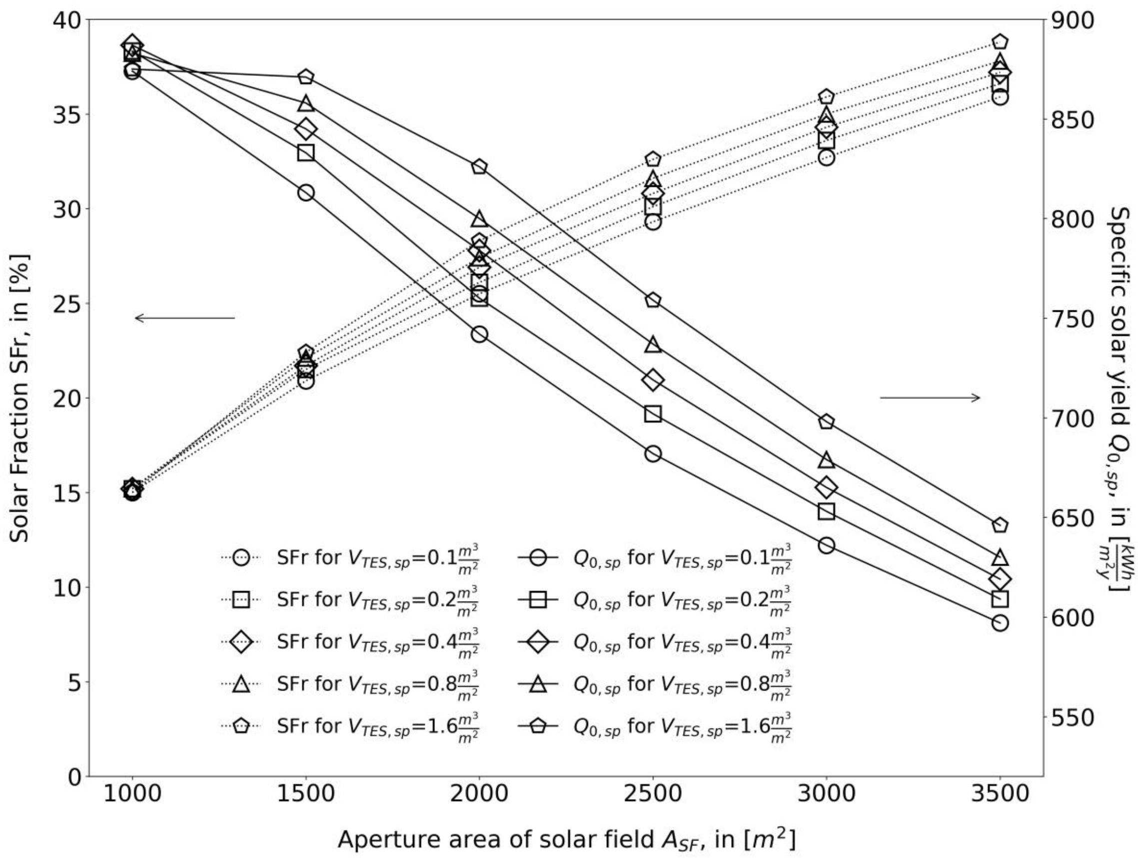

Figure 4: Solar fraction and specific heat productivity for different solar array sizes and specific storage capacities obtained by TRNSYS simulation.

estimating the solar field area required. Once simulated, each configuration has been categorized by the corresponding collector area (A_{SF}, in [m^2]), the resulting specific solar yield ($Q_{0,sp}$ in [kWh/m^2]) and solar fraction (*SFr*, in [%]), and the ratio between the TES volume and the field surface (i.e. or specific TES volume, $V_{TES,sp}$ in [m^3/m^2]). For the different modelled configurations, Figure 4 shows the resulting annual solar fraction and specific productivity as a function of the total field area and the TES specific volume. Solar array size varies between 1000 and 3500 m^2, while the studied range of specific storage capacities is between 0.1 and 1.8 m^3/m^2. As shown, high specific solar productivities are obtained for small solar fractions and small collector areas, as all the solar energy collected in the field can be dispatched to the DHN. For higher solar fractions, in particular during summer and at low load conditions, a larger part of solar energy cannot be readily dispatched to the DHN and needs to be stored in the TES, with increasing production temperatures, or even to be wasted to avoid stagnation. As a consequence, the specific productivity declines. For a given solar field size, furthermore, there exist an optimal value for the specific storage volume above which there is no significant increase in productivity of the solar field, as it can be inferred by the plateau in the specific productivity up to 1500 m^2 at high specific TES volume ratio and its decrease in value from a TES specific volume of 0.8 m^3/m^2 to 1.6 m^3/m^2, shown in Figure 4.

5. Economic analysis

The hybridization of wood-based DH networks with solar thermal energy has several advantages, already mentioned beforehand. But different field-TES combinations have different profitability, which is understandably an important driver of the investment decision-making process. To investigate how the technical features of a solar-hybridization project of an existing biomass plant affect its profitability, an economic model based on discounted cash flow analysis was compiled and a sensitivity analysis on the *LCOH* was carried out. Three scenarios of interest were finally selected for further analysis and the relevant KPI introduced in section 2 were compared.

Table 2: Costs of piping between solar field and DH network

Conduit diameter, in [mm]	Linear cost, in [CHF / m]
80	478
100	616
125	762
150	914
200	1091

Table 3: Assumptions made for the cost calculations related to connection piping.

Parameter	Value
In-pipe water speed, in [m/s]	1
Forward – return temperature difference, in [K]	30
Specific pic power of solar field under nominal conditions, in [W/m^2]	700

5.1 Economic model for KPI calculations

For the purpose of building an economic model and compute the KPI introduced beforehand (i.e, *LCOH*, *PP* and *PI*), only the investments on the solar field, the TES, the control system and the solar piping for connection to the DH were taken into account. Conversely, costs related to adaptations to the wood-fueled boiler circuits, costs or benefits due to wood storage in summer, costs due to land or space acquisition or rent were not taken into account.

The investment and installation costs for the solar field (solar collectors, supports, hydraulic components, control system, heat exchanger, i.e. the solar field CAPEX, noted CAP_{SF}) were estimated with eq. 2, based on private communications with technical partners of the HEIG-VD and for Switzerland.

$$CAP_{SF} = 2682\ A_{SF}{}^{0.826} \qquad \text{(eq. 2)}$$

In eq. 2, CAP_{SF} is the solar field capital expenditure, in [CHF], and A_{SF} the solar field aperture area, in [m^2]. The TES system was estimated, on the other hand, trough eq. 3, as a linear extrapolation of the trend derived from several offers obtained on the Swiss market for off-ground water-based TES tank volumes from 25 up to 300 m^3.

$$CAP_{TES} = 540.9 V_{TES} + 9045.3 \qquad \text{(eq. 3)}$$

In eq.3, CAP_{TES} is the TES capital expenditure, in [CHF], and V_{TES} the TES useful volume, in [m^3].

The costs for the connecting conduits between solar field and DH network were estimated based on values provided by the Swiss Association of DH Networks (ASCAD) shown in Table 2, and based on the assumptions reported by Table 3. To complete the picture, operating expenditures were estimated conservatively by summing up 1%/y of the total solar field CAPEX and the costs due to the electricity consumption of the auxiliary equipment and pumps. Electrical consumption was evaluated by adopting an annual COP value for the solar field of 100 MWh_{th}/MWh_e, about 30% higher than the annual mean encountered on the SolarCADII and reported by Duret et al. (2022). The economic model was completed by a series of assumptions made on the main economic/financial parameters of the model, shown in Table 4.

A sensitivity analysis of 30 cases was carried out with the aim of observing the evolution of the LCOH as a function of the size of the solar array and the storage volume, as shown in Figure 5. The analysis was carried

Table 4: Values adopted for the main parameters of the economic analysis.

Economic model parameter	Value
Solar plant service life, in [y]	25
Solar field yield degradation, in [%/y]	0.8
Solar plant COP, in [MWh_{th}/MWh_e]	100
Electricity price at t=0, in [CHF/MWh]	200
Heat selling price at t=0, in [CHF/MWh]	120
Annual energy price increase, in [%]	3
Nominal discount rate, in [%]	5.2

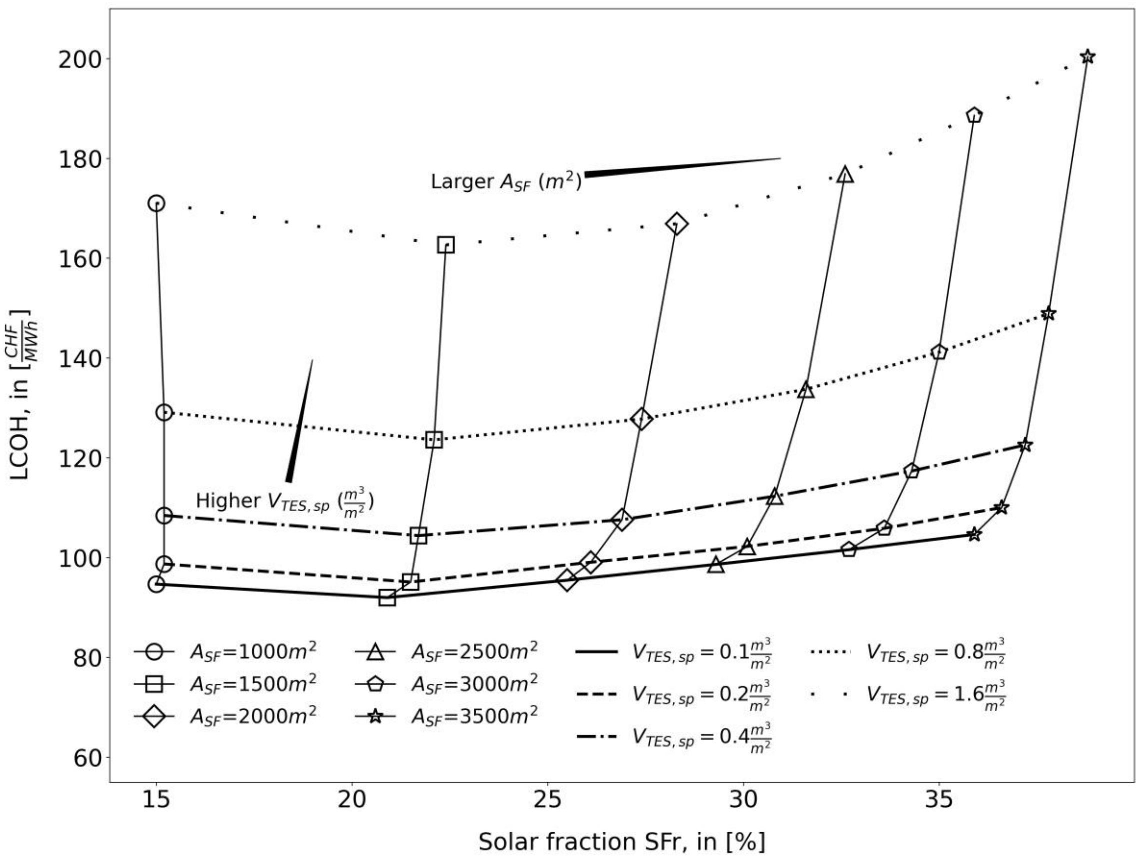

Figure 5: LCOH for a hybrid biomass-solar plant as a function of the solar fraction, the size of the solar array and the storage volume.

out by varying the solar field area in 500 m² steps between 1000 m² and 3500 m², and assuming values for the specific TES volumes of. 0.1, 0.2, 0.4, 0.8 and 1.6 m^3/m^2. As shown in Figure 5, for a given specific TES volume, the LCOH as a function of solar aperture area show a minimum after which any increase in the solar surface is less than optimal. An increase in specific TES volume, on the other hand, affects the LCOH negatively as it is shown from all the curves derived for ratios bigger than 0.1 m^3/m^2. When the increase in the size of the storage volume allows increasing the solar fraction, there are gains in solar heat production but these are offset by the higher investment costs for the purchase of the larger storage. In order to reduce investment and LCOH, it is preferable to opt for small-scale storages.

5.2 Study cases and KPI comparison

In Figure 5, the minimum value of the LCOH for the simulated DH network is found at about 92 CHF/MWh for a solar fraction of about 21%, featured by a 1500 m^2 solar field, equipped with a TES volume of 150 m^3. Three scenarios among those taken into account for the sensitivity analysis were then selected around this optimal case. The three scenarios refer to the same DH network consumption, but they feature differences in solar field area and TES volume. The analysis compared a hybrid plant made of a 1000 m^2 solar field equipped with a 135 m^3 TES to solutions consisting of a 1500 m^2 solar field equipped with 300 m^3 TES and a 2320 m^2 solar field equipped with a 1500 m^3 TES. As such, the scenarios featured specific TES volumes of 0.135, 0.2 and 0.64 m^3/m^2, respectively., while Table 5 shows the values of the main KPIs computed for the three scenarios. As shown, scenario 1 and scenario 2 feature similar values of LCOH, while scenario 3 shows the highest value. This latter scenario, in fact, is equipped with a TES that features a specific volume of about 0.64 m^3/m^2, much higher than the others, whilst also featuring the lowest specific productivity. The much larger size of TES volume allows to cover about 30 % of the energy consumption, but the profitability of the project is affected by its costs, as it is shown by the IRR values evaluated at the heat selling price (including energy inflation) and according to the values shown in section 2.

Table 5: KPI values computed for the three scenarios.

Parameter	Scenario 1	Scenario 2	Scenario 2
Solar field aperture area, in [m^2]	1000	1500	2320
TES Volume, in [m^3]	135	300	1500
Yearly solar yield, in [MWh/y]	855	1'227	1'733
Specific yearly solar yield, in [$kWh/m^2/y$]	855	818	747
Solar fraction, in [%]	14.7	21	29.7
CAPEX, in [CHF]	980'700	1'412'580	2'573'162
LCOH, in [CHF/MWh]	105.3	105.6	135.5
NPV @ selling price, in [CHF]	679'210	968'775	706'304
PP @ selling price, in [y]	12.4	12.5	18.2
PI @ selling price, in [y]	1.69	1.68	1.27
IRR @ selling price, in [%]	11.4	11.3	7.8

5.3 Impact of business model on the LCOH.

Based on the type of adopted business model, the same solution of solar energy integration may have a different economic impact on the overall cost of heat. To address this question, the following two business models were analyzed in reference to the case featuring the lowest value of LCOH:

- The owners of the DH network and plant are members of the rural community and they are reunited as a "Cooperative".
- The DH network and plant are owned by an ESCO (Energy Service Company) external to the rural community.

To evaluate the impact on the energy bill of the DH customers, heat costs from the biomass plant (i.e., 87 CHF/MWh in 2019 for the DHN of " Les-Ponts-de-Martel") and from the solar plant can be weighted according to eq. 4 to estimate the mean heat cost issued by the hybrid plant.

$$LCOH_{mean} = \mathrm{LCOH}_{SF} * SolarFraction + (1 - \mathrm{SolarFraction}) * \mathrm{LCOH}_{biomass} \quad \text{(eq. 4)}$$

In the "Cooperative" case, the aim of the owners is to have the lowest possible cost for the energy that the DH produces and distributes, as they are not interested in a real margin (apart from a small fee meant to pay for operating and managing the energy system). In this case, as there's no interest in having a positive NPV, the LCOH for solar heat can be taken equal to the minimal LCOH (92 CHF/MWh). By assuming 87 CHF/MWh for the biomass heat and 21% for the solar fraction, it can be calculated that the rural community will have access to heat at an average price of 88.05 CHF/MWh. This figure is 1.08 CHF/MWh higher than the biomass-only case, but adding the solar field has many benefits, among others the reduction of the number of cycles featured by the biomass boilers in one year, impacting emissions particularly in summer (Jobard et Duret, 2022).

In the ESCO scenario, on the other hand, the investing and operating entity is a private company, which creates value by charging for the supply of energy to its customers and it is constrained to provide a return to its investors. One may consider, for example, that the ESCO is only willing to invest in projects that have a PP value of 15 years or lower (i.e., corresponding to a heat cost of 128 CHF/MWh). In this case, the solar heat cost is substantially larger than the LCOH, as the ESCO requires a margin to compensate its investors for the risk undertaken and service its debt. In this case, the average selling price for the DH heat can be computed at 95 CHF/MWh. In this latter case, the cooperative would disburse 7-8 CHF/MWh more than for the biomass-only production managed by the Cooperative itself, highlighting the importance of collaboration between stakeholders to achieve balanced financial objectives.

6. Conclusions

This study highlights the technical and financial viability of the integration of solar thermal technology with wood chip boilers. Such an addition can enhance energy efficiency, reduce CO2 emissions, and optimize costs. In particular, it analyses the technical and economic performances of the integration of a large-scale solar thermal field with biomass boilers for district heating (DH) in rural areas, as aligned with the principles of 4th Generation DH for sustainable energy systems. The technical analysis shows that combining solar thermal energy with existing boilers significantly boosts renewable heat production, with a potential optimal solar fraction of about 21 % for the chosen location, Les-Ponts-Des-Martel, a small rural village in Switzerland. Financially, the study confirms that most configurations are economically feasible, with careful consideration of solar field size, storage volume, and associated costs. An optimal TES volume can be identified with respect to the target solar fraction and the surface of the solar field. Two financing scenarios were furthermore explored: one involving cooperative members as investors, which keeps heat costs stable and close to the break-even point, and another with third-party investors, which provides financial gains while maintaining reasonable consumer costs. Overall, the study supports the integration of solar thermal systems, provided that the optimal plant configuration and financing scheme are selected.

7. Acknowledgments

We express our sincere gratitude to the Swiss Federal Office of Energy (SFOE) for their financial support of this research (Project N.SI/502569). and to the cooperative des “Marais-rouge” for providing the DHN data.

8. References

Quiquerez, L., Cabrera S., Jose D., Hollmuller, P., (2013) Températures de distribution de chauffage du parc immobilier genevois. Archive Ouverte UNIGE, https://archive-ouverte.unige.ch/unige:27989.

Lachal, Bernard MarieJenssen, T., König, A., & Eltrop, L. (2014). Bioenergy villages in Germany: Bringing a low carbon energy supply for rural areas into practice. *Renewable Energy, 61*. https://doi.org/10.1016/j.renene.2012.08.014

Klein, S. A., Beckman, W. A., Mitchell, J. W., & Duffie, J. A. (2014). TRNSYS 17 Mathematical Reference. In Trnsys 17 (Vol. 4).

Lund, H., Werner, S., Wiltshire, R., Svendsen, S., Thorsen, J. E., Hvelplund, F., Mathiesen, B. V. (2014). 4th Generation District Heating (4GDH). Integrating smart thermal grids into future sustainable energy systems. In Energy (Vol. 68, pp. 1–11). Elsevier Ltd. https://doi.org/10.1016/j.energy.2014.02.089

Winterscheid, C., Dalenbäck, J. O., & Holler, S. (2017). Integration of solar thermal systems in existing district heating systems. Energy, 137. https://doi.org/10.1016/j.energy.2017.04.159

CEA (2018) D2.3. Key Performance Indicators to evaluate the integration of solar heating in industrial processes; D2.3 SHIP2FAIR ID GA 792276; http://ship2fair-h2020.eu/wp-content/uploads /2018/12/SHIP2FAIR_D2.3_KPI_CEA.pdf

Aldersey-Williams, J., & Rubert, T. (2019). Levelised cost of energy – A theoretical justification and critical assessment. Energy Policy, 124. https://doi.org/10.1016/j.enpol.2018.10.004

Ilie, A., Vişa, I. (2019). Hybrid solar-biomass system for district heating. E3S Web of Conferences, 85. https://doi.org/10.1051/e3sconf/20198504006

Ruesch, F., Caflisch, M., Haller, M. (2020). BioSolFer Integration von Solarwärme in Biomasse Fernwärmenetze, www.ost.ch/fileadmin/dateiliste/3_forschung_dienstleistung/institute/spf/forschung/projekte/biosolfer_schlussbericht_2020.pdf

Tschopp, D., Tian, Z., Berberich, M., Fan, J., Perers, B., Furbo, S. (2020). Large-scale solar thermal systems in leading countries: A review and comparative study of Denmark, China, Germany and Austria. Applied Energy, 270(January), 114997. https://doi.org/10.1016/j.apenergy.2020.114997

Duret, A., Jobard, X., Pauletta, S., Demonchy, G. (2022). Performance Monitoring of an 800m^2 Solar Thermal

Plant with Evacuated Flat Plate Collectors coupled to a DHN. Proceedings of EuroSun 2022 - ISES and IEA SHC International Conference on Solar Energy for Buildings and Industry, 1–10. https://doi.org/10.18086/eurosun.2022.04.02

Hiris, D. P., Pop, O. G., & Balan, M. C. (2022). Preliminary sizing of solar district heating systems with seasonal water thermal storage. Heliyon, 8(2). https://doi.org/10.1016/j.heliyon.2022.e08932

Jobard, X., Duret, A. (2022). Operability of District Heating Plants Combining a Large-Scale Solar Thermal Field and Condensing Wood Chip Boilers – a Case Study in Switzerland. Proceedings of EuroSun 2022 - ISES and IEA SHC International Conference on Solar Energy for Buildings and Industry, 1–11. https://doi.org/10.18086/eurosun.2022.04.03

Jodeiri, A. M., Goldsworthy, M. J., Buffa, S., & Cozzini, M. (2022). Role of sustainable heat sources in transition towards fourth generation district heating – A review. In *Renewable and Sustainable Energy Reviews* (Vol. 158). https://doi.org/10.1016/j.rser.2022.112156

Duret, A., Jobard, X., Pauletta, S., Lasvaux, S., Frossard, M., Demonchy, G. (*in press*). Dynamic Simulation and Life Cycle Analysis of a 784m^2 Solar Thermal Plant with Evacuated Flat Plate Collectors coupled to a DHN. J. Thermal Sciences.